



1 **Water Vapor Retrieval using the Precision Solar Spectroradiometer**

2

3 **Raptis Panagiotis-Ioannis^{1,2}, Kazadzis Stelios¹, Gröbner Julian¹, Kouremeti**
4 **Natalia¹, Doppler Lionel³, Becker Ralf³, Helmis Constantinos²**

5

6 ¹*Physikalisch-Meteorologisches Observatorium Davos-World Radiation Center (PMOD-WRC),*
7 *Davos, Switzerland*

8 ²*University of Athens, Department of Physics, Athens, Greece*

9 ³*Deutscher Wetterdienst, Meteorologisches Observatorium Lindenberg – Richard Assmann*
10 *Observatorium (DWD, MOL-RAO), Lindenberg (Tauche), Germany*

11

12

13

14 **Abstract.**

15 The Precision Solar SpectroRadiometer (PSR) is a new spectroradiometer developed at
16 Physikalisch-Meteorologisches Observatorium Davos-World Radiation Center (PMOD-WRC),
17 Davos, measuring Direct Solar Irradiance at the surface, in the 300-1020 nm spectral range at
18 high temporal resolution. The purpose of this work is to investigate the instrument's potential
19 of retrieving Integrated Water Vapor (IWV) using its spectral measurements. Two different
20 approaches were developed in order to retrieve IWV, the first one using single
21 channel/wavelength measurements, following a theoretical water vapor high absorption
22 wavelength, and the second one using direct sun irradiance integrated at a certain spectral
23 region. IWV results have been validated using a 2-year dataset, consisting of an AERONET sun-
24 photometer Cimel CE318, a Global Positioning System (GPS), a Microwave Radiometer
25 Profiler (MWP) and radiosonde retrievals recorded at Meteorological Observatorium
26 Lindenberg, Germany. For the monochromatic approach, better agreement with retrievals
27 from other methods/instruments was achieved using the 946nm channel, while for the
28 spectral approach using the 934-948 nm window. Compared to other instruments' retrievals,
29 the monochromatic approach leads to mean relative differences up to 3.3% with the
30 coefficient of determination (R^2) being in the region of 0.87-0.95, while for the spectral



1 approach mean relative differences up to 0.7% were recorded with R^2 in the region of 0.96-
2 0.98. Uncertainties related to IWV retrieval methods were investigated and found to be less
3 than 0.28cm for both methods. Absolute IWV deviations of differences between PSR and
4 other instruments were determined the range of 0.08-0.30 cm and only in extreme cases
5 would reach up to 15%.

6
7

8 **1.Introduction**

9 Water Vapor is a very important component of the thermodynamic state of the atmosphere
10 (Hartman et, al 2013), being a greenhouse gas with relatively high concentrations. The
11 quantity of water in the vapor state depends on temperature. So, from a climate change
12 perspective, it is considered as a feedback agent (Soden and Hled, 2006). Also, it is an
13 important component of the hydrological cycle and estimations of it are used in
14 meteorological forecast models (eg. Hong et al., 2015, Bock et al., 2016). Finally, a robust
15 estimation is needed to study microphysical processes that lead to the formation of clouds
16 and determine their composition (water droplets or ice crystals) as well as the statistical
17 shape and size of these components (Reichard et al., 1996, Yu et al., 2014).

18 IWV in the vertical atmospheric column is a very common variable in meteorological and
19 climatological studies. It is defined as the height that water would stand if completely
20 condensed and collected in a vessel of the same unit cross section (American Meteorological
21 Society, 2015). Monitoring of water vapor in the atmosphere has been performed through
22 radiosondes and provided through measurements of vertical profiles of humidity. These
23 measurements are limited to relatively infrequent (radiosonde) launches; thus, during the last
24 decades there have been developed methods to retrieve IWV from other devices:

- 25 • Continuous monitoring of IWV is established through Global Positioning System (GPS)
26 satellite observations (Bevis et al., 1992), which could be used to retrieve IWV
27 anywhere in the globe at relatively high temporal frequencies. The theoretical basis
28 for these measurement is that delays in the signals emitted by GPS satellites are
29 caused by the amount of water in the atmosphere, and through proper calibration,
30 such delays could be expressed as function of the IWV. Thus, as long as there are
31 ground based GPS receivers, after the appropriate post-processing of the received
32 signals, IWV can be retrieved.



- 1 • Microwave Radiometer Profilers (MWP) measure the emitted microwave radiation of
2 the atmosphere and retrieve water vapor vertical profiles and then IWV, providing
3 continuous data at very high frequencies under all weather conditions (e.g. Güldner
4 and Spankuch, 2001, Güldner, 2013). These instruments provide very high accuracy
5 but are not very common.
- 6 • Measurements from sun-photometers have also been used to calculate water vapor
7 transmittance and, thus, estimate IWV. Filter radiometer recordings in the spectral
8 region around water vapor absorption bands, in the near infrared region, are used to
9 calculate this quantity. The World Meteorological Organization (WMO) recommends
10 the use of spectral windows centered around 719, 817 and 946 nm, though the most
11 frequently used is the 946 nm bandpass, which Ingold et al. (2000), showed that
12 provides the most robust results.

13

14 Global networks of deployed sun-photometric devices are capable of providing IWV time
15 series. The AERosol RObotic NETwork (AERONET) retrieves IWV at more than one hundred
16 stations around the globe since the 1990's (Holben et al. 1998,
17 <https://aeronet.gsfc.nasa.gov/>) using the Cimel instrument. Other sun-photometers such as
18 the Precision Filter Radiometers (PFR) (Nyeki et al., 2005) have also been used by the Global
19 Atmosphere Watch (GAW) WMO program to monitor IWV. Furthermore, the SKYNET
20 radiometer network (details on: <http://atmos2.cr.chiba-u.jp/skynet/>) also retrieves IWV using
21 Prede-POM sunphotometers at many stations (Campanelli et al., 2012, 2014). Finally, national
22 networks of sunphotometers are installed and operating in some countries also provide IWV
23 retrievals, eg. China Aerosol Remote Sensing NETwork (CARSNET) is using the 936nm channel
24 to provide IWV (Che et al., 2016).

25 Schneider et al. (2010) provided a very detailed comparison of different instrument retrievals
26 over a 4-year data set recorded at Izaña Atmospheric Observatory, Tenerife, Spain. They
27 found that MWP is the most precise technique and, in addition, it is independent of weather
28 conditions, while sun-photometric retrievals were limited by cloudy and biased by dry/humid
29 atmospheres, and GPS retrieved IWV showed deviations at lower IWV values. Deviations were
30 also recorded when compared to radiosondes, which was explained by the difference in air
31 masses and time scales among radiosondes and other IWV retrievals.



1 Technological advances of the recent years have made feasible the manufacturing of
2 operational spectral sun-photometers for environmental monitoring. The Precision Solar
3 Spectroradiometer (PSR), designed and manufactured at PMOD/WRC, Davos, Switzerland, is
4 one of the most accurate instruments of this class (Gröbner et al., 2012). In this study we
5 have developed tools to retrieve IWV using PSR recordings, adopting two different
6 approaches; one using single wavelength channels and another retrieving from a wider
7 spectral region, the latter being impossible with filter radiometers. Retrievals in different
8 channels and spectral windows in the water vapor absorbing region of near infrared spectrum
9 were evaluated and selected. Both methods were applied to a 2-year long PSR dataset at the
10 German Meteorological Service (Deutscher Wetterdienst, DWD) site in Lindenberg, Germany
11 and results have been compared with sun-photometric (CIMEL), GPS, radiosonde and MWP
12 IWV datasets from the same station.

13

14 **2. Instrumentation**

15 Methodologies for retrieving IWV were applied to PSR measurements at *Meteorologisches*
16 *Observatorium Lindenberg – Richard Assmann Observatorium* (MOL-RAO) from the German
17 Meteorological Service “Deutscher Wetterdienst” (DWD) in Lindenberg (Tauche), in the
18 North-East Germany (52° 12' N, 14° 7' E), where a 2-year long PSR dataset is available (May
19 2014- April 2016). MOL-RAO is a supersite for measurements of aerology and radiation, thus
20 it provides a variety of collocated measurements that could be used for validation. MOL-RAO
21 is exclusively devoted to instrumental measurements of the atmosphere and a numerous
22 technical staff guarantees daily maintenance of the instruments. All instruments and
23 corresponding techniques are described below. Sunshine at the area ranges from 55
24 hours/month at December to 256 hours/month during summer months on average; also,
25 rain is recorded almost for 1/3 of days during all 12 months (Beyrich and Adam, 2005).
26 Minimum solar zenith angle (SZA) reaches 30° during summer months while during winter it
27 is over 70°. AOD is generally very low in the area, with maximum mean monthly values of
28 0.25 and 0.27 during June and July.

29

30 **2.1 PSR**

31 A new generation of solar spectroradiometer, the Precision Solar Spectroradiometer (PSR), is
32 being developed at PMOD/WRC in order to eventually replace current filter sun-photometers.



1 It is based on a grating monochromator of stabilized temperature with a 1024 pixel
2 Hamamatsu diode-array detector, operating in a hermetically sealed nitrogen-flushed
3 enclosure. The spectroradiometer is designed to measure the solar spectrum within the 300
4 to 1020 nm wavelength range with an average step of ~ 0.7 nm and spectral resolution from
5 1.5 nm to 6 nm (full width at half maximum, depending on the measured wavelength). The
6 design benefits from the experience gained from successive generations of the successful
7 Precision Filter Radiometers (PFR), including: an in-built solar pointing sensor, an ambient
8 pressure sensor and temperature sensors to provide routine quality control information,
9 which allows autonomous operation at remote sites with state-of-the-art data exchange via
10 Ethernet interfaces. The PSR used in this study is the PSR#006, which is installed on the MOL-
11 RAO site. This instrument has been calibrated at PMOD/WRC using a 1000 W transfer
12 standard lamp source, in May 2014 and October 2015. A comparison between the two
13 calibrations showed relative differences less than 1% for most spectral channels and more
14 than 2% only in the region above 980 nm (Kouremeti et al., 2015). Moreover, stray light
15 corrections have been applied and absolute direct and global (horizontal) Irradiance time
16 series are available for all 1024 available channels (Gröbner et al., 2014).

17

18

19 **2.2 CIMEL Sun-photometer**

20 The CIMEL sun-photometer is a filter radiometer developed by Cimel Electronics (Paris,
21 France), which performs direct sun and sky radiance measurements. These measurements
22 are processed centrally and are widely available through AERONET (Holben et al., 1998).
23 Measurements are performed at eight bandpass filters between 340 and 1064 nm. Direct
24 measurements are performed usually every 10-15 minutes. Direct sun measurements at 940
25 nm are used to retrieve IWV. At this channel the Full Width Half Maximum is 10 nm, (Schmid
26 et al., 2001) which means that the solar signal recorded represents a relatively wide spectral
27 region. The method used to retrieve it is described in detail in Smirnov et al. (2004). The
28 principle of this method is to calculate a two constants' fit, using radiative transfer model
29 calculations in order to retrieve IWV from the transmittance recorded at 940 nm. The
30 precision of this retrieval was investigated by Alexandrov et al. (2009) who showed an error
31 in the region of 0.05-0.18 cm depending on the amount of IWV.



1 The CIMEL Level 2 AOD data for MOL-RAO has been directly downloaded from AERONET
2 website (<https://aeronet.gsfc.nasa.gov/>). During the 2 years of this study, the station has
3 been equipped with three different instruments:
4 - Cimel CE318N, #787
5 - Cimel CE318N, #873 supplying #787 during its AERONET calibration
6 - Cimel CE318T (“Triple”) since October 2015, instrument of higher temporal resolution
7 (~ 1 minute)

8 9 **2.3 Global Positioning System**

10 GPS is a space based system that uses the signal transmitted from specific satellite
11 instrumentation in order to define the geolocation of ground based receivers. The signal
12 delays could be separated into dry (dependent on dry air gases) and wet (water vapor)
13 component. Although the biggest fraction of the delay is caused by the dry component, it is
14 estimated by hydrostatic equations, using the surface pressure, and subtracting it from the
15 total delay. This is considered a very accurate retrieval of the wet component, to which IWV
16 is directly proportional (Bevis et al, 1992). Wang et al. (2007) showed that the random error
17 of GPS IWV retrievals is in the order of 0.7 mm. GPS IWV retrievals are very valuable, since
18 this method could be applied to any receiver and obtain a very reliable and dense dataset of
19 frequent observations, both for daytime and night time, without being affected by cloud
20 conditions. Differences among GPS and sun-photometric retrievals are expected, as different
21 optical paths are used in each case and different air masses are detected: GPS path is a quasi-
22 random path depending on the position of the satellites while the sun-photometer path is
23 defined by the sun-instrument’s relative positions.

24 25 **2.4 Microwave Radiometer Profiler**

26 At MOL-RAO, a 22-channel MWP, MP-3000A /Radiometrics (Ware et al., 2003) provides
27 vertical temperature and humidity profiles. In principle, observations from these instruments
28 are based on recording the down-welling thermal emission of the atmosphere in the region
29 between 22 and 30 GHz, using a zenith sky looking sensor. A full description of the Water
30 Vapor retrieval methodology of MWP could be found at Westwater et al. (2005). Cadeddu et
31 al. (2013) have estimated the uncertainty of this technique in the order of 5% for IWV less
32 than 10mm.



1

2

3 **2.5 Meteorological Radiosonde**

4 Meteorological radiosondes (RS) are launched in many places around the world, recording
5 vertical profiles of various meteorological variables (Temperature, Wind Speed, Humidity
6 etc). Water Vapor profiles provided by the soundings can be used to calculate IWV. This is the
7 most objective approach for validating ground based remote sensing techniques, since water
8 vapor is measured in-situ during the ascending procedure. Uncertainty for IWV retrieval in
9 this approach is introduced by the nature of the method, as the total ascending of a
10 radiosonde to stratosphere takes approximately an hour and also the path of the radiosonde
11 in the atmosphere is determined by winds; thus, it is not directly comparable to sun-
12 photometric estimations, which retrieve water vapor on the sun-point of observation optical
13 path. High uncertainties -up to 20%- for relative humidity, caused by warming due to sunlight
14 and thermal lag, have been reported (Pratt, 1985). Also, studies have reported differences
15 due to the use of different sensors (e.g. Soden and Lanzante 1996). Vaisalla RS92 radiosondes
16 are used in this study for which an uncertainty in the order of 5% for the RH (Relative
17 Humidity) measurements, during daytime in the Troposphere, has been reported
18 (Miloshevich et al.,2009). Radiosondes from MOL-RAO are launched 4 times per day (00h,
19 06h, 12h, 18h UTC). So, for this study 1-3 daytime soundings, per day, can be used, depending
20 on the season. Corrections, as suggested by Vömel et al. (2007) for the dependence of the
21 humidity sensor on temperature and radiation, were applied.

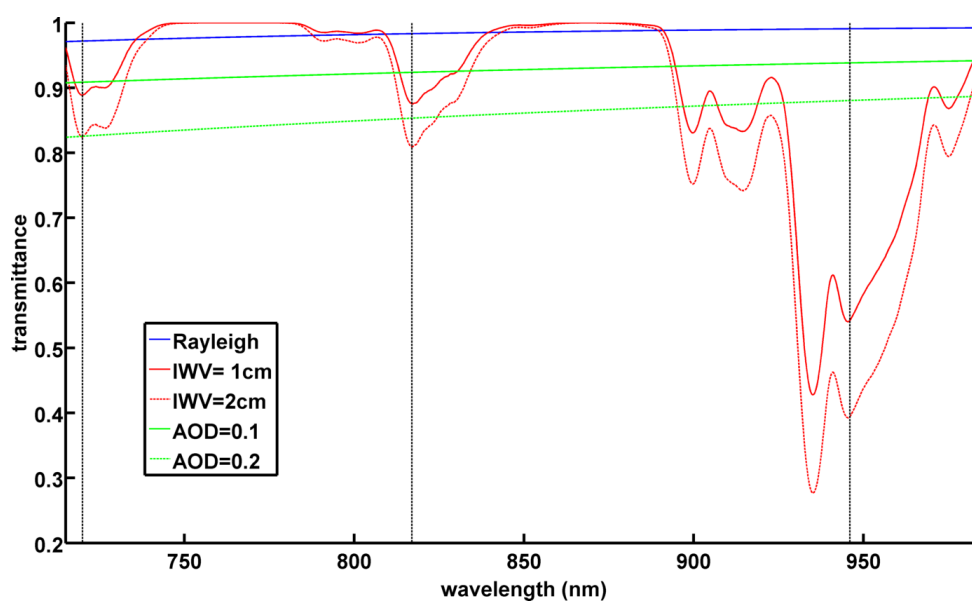
22

23 **3. Methodology**

24 In the near infrared measuring spectral region of PSR the most important water absorption
25 has been found in the 700-1000 nm wavelength region. Figure 1 shows the transmittance
26 from Rayleigh scattering, aerosols and IWV, as calculated by the MODerate resolution
27 atmospheric TRANsmisson Radiative Transfer Model (MODTRAN RTM) (Berk et al., 1987, Berk
28 et al., 1999). Aerosols direct effect on irradiance is measured through Aerosol Optical Depth
29 (AOD) which is the integrated extinction coefficient on vertical column due to aerosols.
30 Spectral variation of AOD at different wavelengths is measured through Ångström Exponent.
31 For the example on figure 1, Ångström Exponent equal to 1.5 was considered and aerosol of
32 AOD 0.1 and 0.2. Inclination of aerosol transmittance lines is proportional to Ångström



1 Exponent and higher AOD will lead to lower absolute values. WMO (2004) recommends 719,
2 817 and 946 nm central wavelengths to retrieve IWV, which appears as significant drops in
3 the solar transmittance spectra in Figure 1. Ingold et al. (2000) investigated the quality of the
4 retrievals at these wavelengths and found that the one at 946 nm is the most robust, which
5 could be translated as the wavelength range with the strongest absorption of IWV.
6 Considering that absorption of water vapor is higher in the 910-950 nm region, all calculations
7 were performed for PSR channels in the spectral range.



8
9

10 **Figure 1.** Transmittance of Water Vapor, Aerosols and Rayleigh scattering in the spectral
11 region 700-1000 nm, calculated using MODTRAN set at 0.1 nm resolution, at $SZA=0^\circ$
12 $IWV=1cm$, $IWV=2cm$ and $AOD=0.1$ and $AOD=0.2$ at 700nm using an Ångström Exponent of
13 1.5. Black vertical dotted lines represent WMO recommendations for IWV retrieval.

14

15 3.1 Monochromatic Approach

16 The methodology in use is described in detail by Ingold et al. (2000) and it is the most
17 common procedure to calculate IWV for sun-photometric devices using individual wavelength
18 (filter) measurements. It is labeled as monochromatic in contrast to the second approach
19 presented in 3.2, although it is calculated for a spectral region defined by the instrument's slit
20 function or the limits of its bandpass filter.



1 The first step of the procedure is to calculate the Water Vapor transmittance T_w in the spectral
2 window of use and afterwards to develop empirical formulas using RTM calculations to
3 determine the IWV from the calculated transmittance.

4 For specific spectral regions in the near infrared, where absorption of dominant trace gases
5 can be considered negligible, we can express the transmittance of the Atmosphere (T_{atmo}) as
6 follows:

7
8
$$T_{atmo} = \frac{I_\lambda}{I_{0,\lambda}} \quad (1)$$

9
10 where I_λ is the recorded spectral irradiance at wavelength λ (in $\text{Wm}^{-2}\text{nm}^{-1}$) and $I_{0,\lambda}$ is the value
11 of the solar irradiance at the top of the atmosphere at the same wavelength.

12 We can express the Beer-Lambert law with respect to water vapor transmittance as follows:

13
14
$$T_{atmo} = e^{(-m_{ray}\tau_{ray,\lambda} - m_a\tau_{a,\lambda})} * T_w \quad (2) \rightarrow$$

15
16
$$T_w = \frac{I_\lambda e^{(m_{ray}\tau_{ray,\lambda} + m_a\tau_{a,\lambda})}}{I_{0,\lambda}} \quad (3)$$

17
18 where T_w is the transmittance of water vapor, τ_{ray} is the Rayleigh scattering optical depth, τ_a
19 is the aerosol optical depth (AOD), m is the relative optical air mass of aerosol and Rayleigh
20 scattering accordingly. For the Rayleigh scattering cross-section we have used the formula
21 found at Bodhaine et al. (1999).

22 Also, for $I_{0,\lambda}$ we have used extraterrestrial values calculated for each of the PSR wavelengths
23 measured as presented by Gröbner et. al. (2017a, 2017b). Spectral AODs were calculated
24 using the Beer-Lambert law and the above extraterrestrial solar spectrum (Kouremeti and
25 Gröbner, 2012). For calculating AOD at the wavelengths in the 920-950nm region, where
26 direct sun measurements are affected by water vapor, we have applied a least square
27 quadratic spectral extrapolation, using $\ln(\text{AOD})$ as function of $\ln(\text{wavelength})$ and the PSR
28 AODs at 500 - 865 nm following Eck et al. (1999) suggestion for AERONET retrievals.

29 In order to convert T_w into IWV we have used the three-parameter expression found in Ingold
30 et al. (2000):

31



1 $T_w = ce^{-a\chi^b}$ (4)

2

3 where

4

5 $\chi = \frac{u m_w}{u_0}$ (5)

6

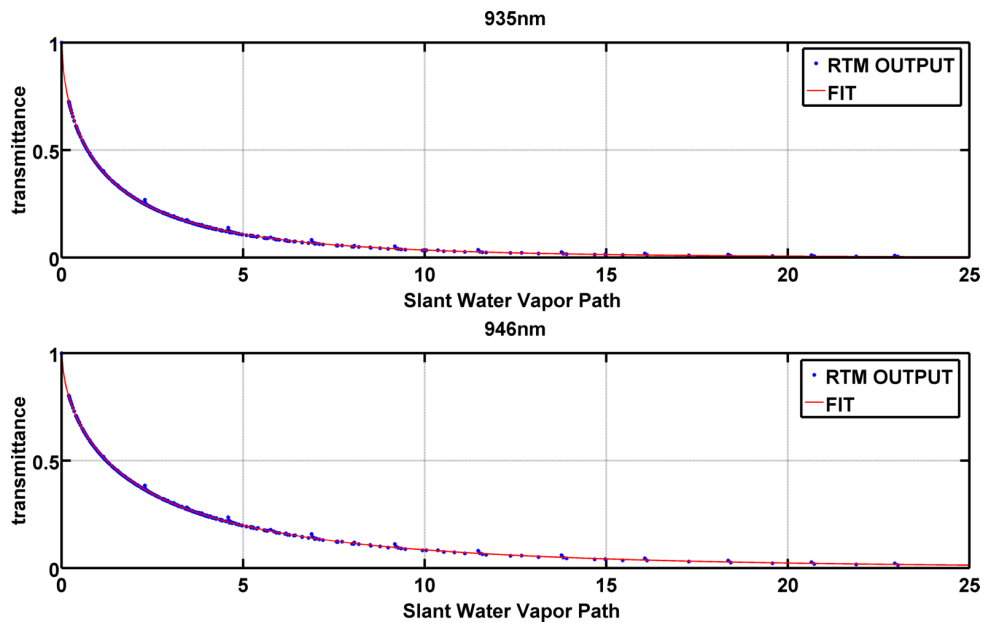
7 with $u_0 = 10 \text{ kg/m}^2$, u representing IWV, m_w as the H_2O air mass and a, b, c the three
8 wavelength dependent coefficients. At this step the coefficients of equation (4) can be
9 estimated. For that purpose, we have used MODTRAN multiple runs for solar zenith angle
10 (SZA) in the region of 0° to 85° with steps of 2.5° . We have used the mid-latitude built in
11 model atmosphere, in the spectral region 0.7 to $1.0 \mu\text{m}$ and IWV from 0 to 40 mm with steps
12 of 2 mm for site elevation set at 110m (MOL-RAO). The modeled spectra were convolved by
13 the spectrally dependent instrument slit function in order to derive comparable (model-PSR)
14 results. Then T_w retrieved from the output spectra was calculated as a function of Slant Water
15 Vapor Path ($m_w \cdot u$), and a fit of these values is used to estimate the coefficients (a, b, c) of
16 equation (4). This procedure was repeated for all PSR channels in the whole spectral region
17 of $900\text{-}950 \text{ nm}$. In figure 2 we present these fits for wavelengths 935.5 and 946 nm . Fits for
18 wavelengths lower than 926 nm were unsatisfactory ($R^2 < 0.7$), suggesting that a different
19 parameterization should be used in this area instead of equation (4).

20 After determining the coefficients a, b, c , equations could be solved in order to calculate the
21 IWV :

22 $IWV = \frac{1}{m_w} \left(\frac{\ln(T_w/c)}{-a} \right)^{1/b}$ (6)

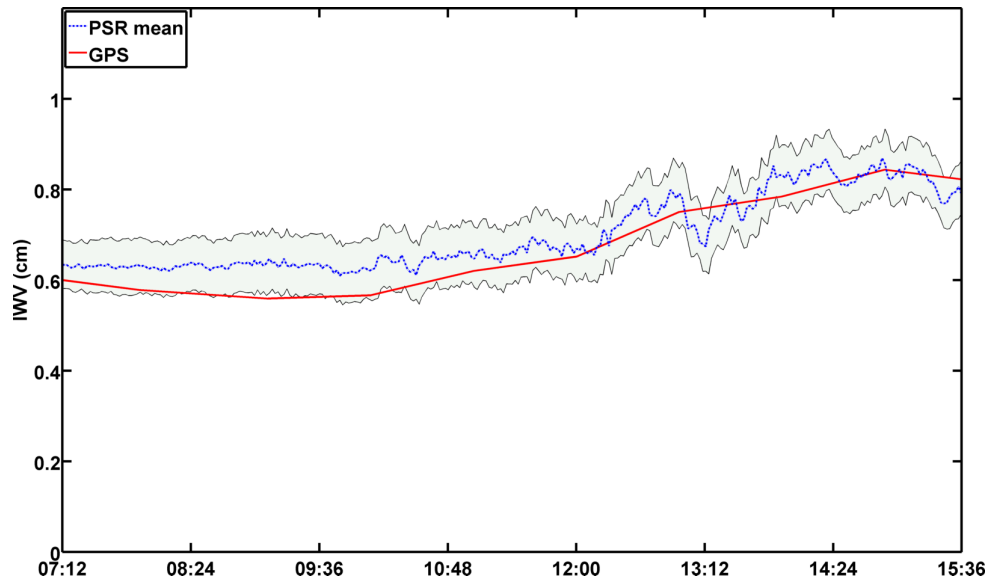
23

24 Thus, IWV now depends only on T_w and air mass, although the coefficients depend on the
25 altitude of the measurement site; so, different RTM runs are needed for each installation.



1
2 **Figure 2.** Transmittance of IWV versus Slant Water Vapor Path ($m_w \cdot u$) calculated by
3 MODTRAN, and three-parameters expression fit for 935 and 946nm bandpasses.

4
5 In order to test the above methodology, we have retrieved IWV on September 30th, 2015, for
6 each PSR channel in the 920-950 nm region separately, after calculating wavelength
7 dependent a , b , and c coefficients. Also, aerosol and Rayleigh transmissions were calculated
8 separately for each wavelength. An average value of all wavelengths in the regions 920-
9 948nm is shown in Figure 3 for one day alongside with GPS IWV retrievals. The standard
10 deviation of the residuals retrieved from different wavelengths is 0.11. The IWV retrievals at
11 946 and 935.5 nm have the smallest deviations compared to the GPS and CIMEL retrievals,
12 because at these wavelengths the absorption due to water vapor absorption is higher. At
13 these two wavelengths, the agreement with CIMEL measurements is very good, with
14 correlations (expressed as the R^2 coefficient) of 0.94 and 0.93 respectively. The lowest R^2 is
15 found for wavelengths shorter than 928 nm which is in the order of 0.6. At figure 3 the mean
16 IWV from all wavelengths for one day (30 September 2015) is presented as an example,
17 alongside with the standard deviation of all monochromatic retrievals. The standard deviation
18 of the residuals retrieved from different wavelengths is 0.11. Following WMO guidelines, we
19 decided to use retrievals at 946 nm for this study and the monochromatic approach.



1 07:12 08:24 09:36 10:48 12:00 13:12 14:24 15:36
 2 **Figure 3.** Retrievals of monochromatic approach on 30th September 2015 at various
 3 wavelengths. Average IWV retrieved using the monochromatic approach at different
 4 wavelengths represented by blue line; the shaded area represents the standard deviation (1σ)
 5 of retrievals at different wavelengths, and the red curve represents the IWV retrieved from
 6 GPS.

7
 8

9 **3.2 IWV retrieval using integrated spectral windows**

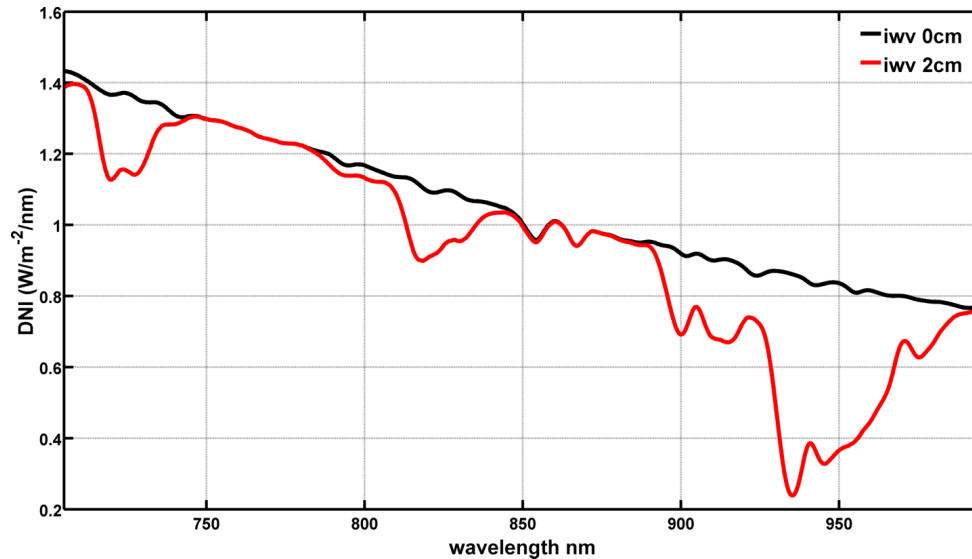
10 In order to benefit from the high resolution spectral measurements available from the PSR
 11 we developed a method that uses direct sun integrated irradiances for a spectral window in
 12 contrast to individual/single wavelengths as previously described. This methodology is
 13 expected to improve the IWV retrieval, since the large variability found in the IWV retrievals
 14 at different wavelengths suggests that an approach that combines different wavelengths
 15 could possibly be more accurate. Figure 4 shows two theoretical spectra in the region of 700-
 16 1000 nm (calculated using MODTRAN), at SZA=0° with no aerosol load and with 0 and 2 cm
 17 of IWV respectively. In this approach we have used the transmittance of the whole spectral
 18 window, and then equation (3) can be written as follows:

$$19 \quad T_{w,\Delta\lambda} = \frac{\int_{\lambda_1}^{\lambda_2} I(\lambda) \exp(m_{ray}\tau_{ray}(\lambda) + m_a\tau_a(\lambda)) d\lambda}{I_0(\lambda) \Delta\lambda} \quad (7)$$

20



1 Where λ_1 and λ_2 are the area wavelength limits, and $\Delta\lambda=\lambda_2-\lambda_1$.



2

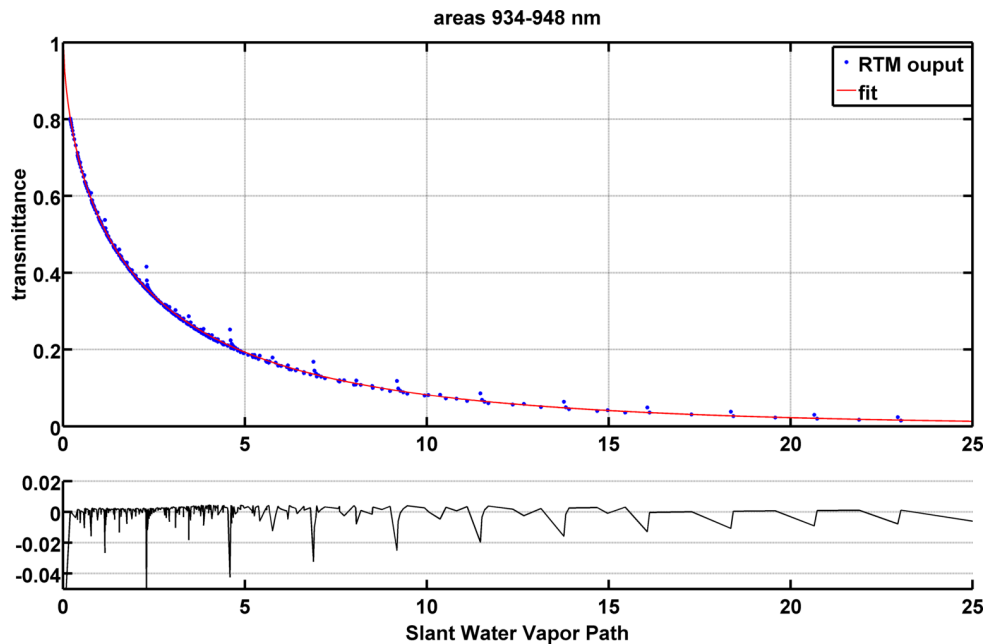
3 **Figure 4.** Calculated Spectra of Direct Solar Irradiance, at $SZA=0^\circ$ with $AOD=0$ and $IWV=0$ cm
4 (black) and 2 cm (red), as calculated from MODTRAN RTM.

5

6 A similar methodology for converting transmittance to IWV, as in the monochromatic
7 approach described above is applied again in order to calculate a third order polynomial
8 function, valid for the wide spectral region. The same MODTRAN outputs were used as in the
9 monochromatic approach but integrated over each spectral window, and the coefficients for
10 equation (4) were calculated accordingly. Calculations have been performed for spectral
11 windows with variable wavelength limits. An investigation on the selection of spectral
12 window has been performed because, as monochromatic retrievals suggested (figure 3), the
13 IWV calculation depends on the wavelength region in use. This investigation was made by
14 changing the window, keeping the upper limit fixed at 948 nm and having the lower one
15 varying between 930 to 946 nm with a step of 1 nm. This selection was made based on the
16 water vapor absorption features as shown in Figure 4, so that the spectral window always
17 includes the high absorption region of 943-947 nm. Longer than 947 nm wavelengths were
18 avoided as there were higher uncertainties in the PSR calibration (Kouremeti et al., 2015,
19 Gröbner et al., 2017). As demonstrated in Figure 4 (for the 934 - 948 nm window), fitting of
20 the 3-parameter equation had results of similar statistics with the monochromatic approach



- 1 in that region. Residuals from fitting at this window are at average at 0.007 but there are also
- 2 some up to 0.04. So, for each spectral window a new 3-parameter function is calculated.



3
 4 **Figure 5.** *Integrated Transmittance of IWV in the 934-948 nm window versus Slant Water*
 5 *Vapor Path ($m_w * u$) calculated by MODTRAN, and Third order polynomial fit.*

6
 7 In figure 6 results from different spectral windows have been compared to other instruments'
 8 retrievals for the whole MOL-RAO dataset. The coefficient of determination R^2 has been used
 9 to evaluate the performance of the spectral approach at different spectral windows, and was
 10 calculated as below:

$$11 \quad R^2 = 1 - \frac{\sum_i (y_i - f_i)^2}{\sum_i (y_i - \langle y \rangle)^2} \quad (8)$$

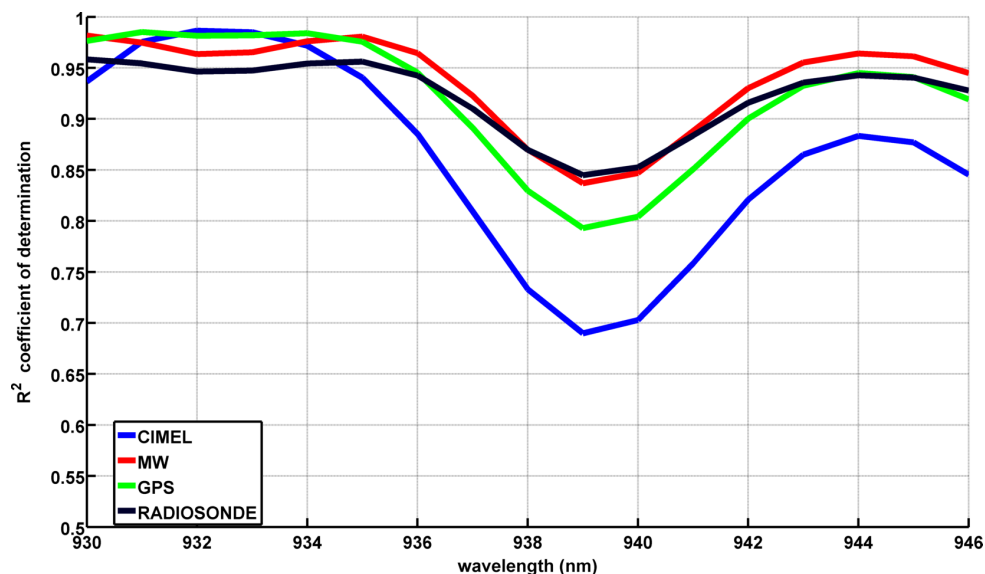
12 where y_i are the IWV values from the other instruments (CIMEL, MW, GPS, RS), $\langle y \rangle$ is the
 13 average of those values and f_i are the IWV values from PSR.

14 Horizontal axis of figure 6 represents the lower limit of the spectral window, the higher being
 15 always fixed at 948 nm. The aim of this step is to find out which spectral window produces
 16 the more robust IWV retrieval results. These comparisons suggest that different spectral
 17 windows selection lead to different coefficients of determination for IWV retrieval compared
 18 with different instruments. However, results converge to defining a lower wavelength limit



1 between 932 and 936 nm. The window 934-948 nm was selected to be used for further
2 analysis.

3
4



5

6 **Figure 6**, IWV retrievals from PSR using spectral approach with different spectral windows,
7 using fixed upper boundary at 946 nm and moving lower boundary at x axis, compared to
8 synchronous ones of CIMEL, GPS, MWP and radiosonde, for the full 2-year measuring period.

9

10 It is interesting to observe different R^2 of the PSR IWV retrievals as compared using different
11 instruments. Especially the fact that by minimizing the spectral window the R^2 s decrease
12 showing a minimum of at window 939-946 nm. For this particular range all R^2 s are below
13 0.85 with the one of CIMEL-PSR showing a minimum. The differences observed when
14 comparing the PSR using different instruments can be partly explained based on the results
15 of section 5.

16

17 **4. Uncertainty budget of IWV retrievals**

18

19 Uncertainty estimation of the IWV retrieval is very crucial for evaluating our comparing
20 results. Beginning from equations (3) and (7) and the calculations of T_w , errors as introduced



1 from each variable are estimated and their propagation to the total uncertainty of IWV
2 retrieval is calculated.

$$3 \quad T_w = \frac{I_\lambda e^{(m_{ray} \tau_{ray, \lambda} + m_a \tau_{a, \lambda})}}{I_{0, \lambda}} \quad (3)$$

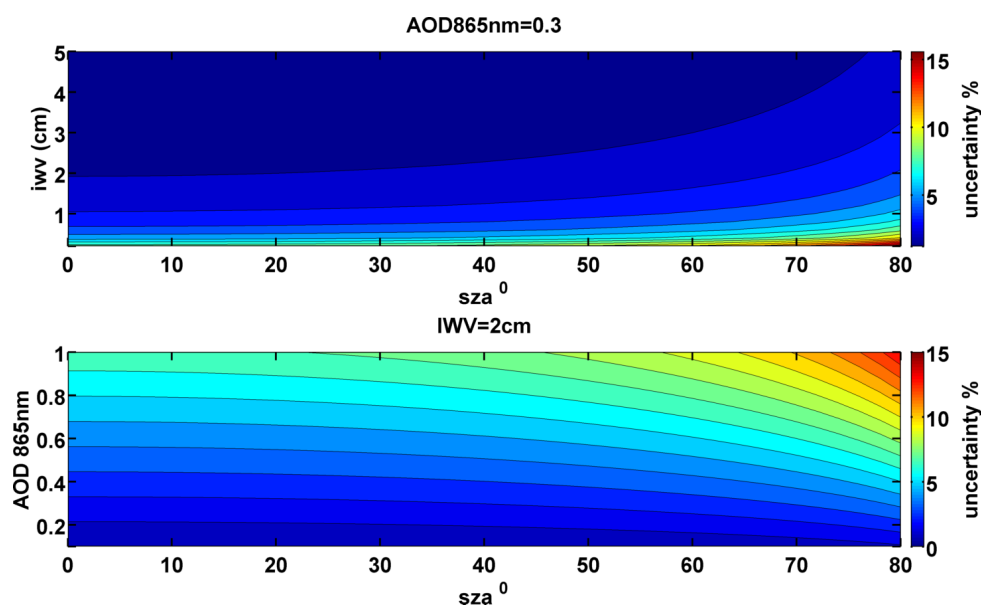
4

5

6 From equation (3), the term that introduces the higher uncertainty in the retrieval of the IWV
7 through the use of Beer-Lambert law is the AOD. A benefit from the methodology applied in
8 this case is that the same set of I_o are used for calculating T_w and AOD, and so errors related
9 to the determination of I_o do not propagate in the calculations. PSR AOD retrievals at 865 nm
10 have been found in accordance with prototype PFR triad when compared during FRC IV, 2015
11 (Filter Radiometer Comparison (GAW, 2016)) with average AOD differences at 865nm less
12 than 0.02. Also, a calibration stability study of the PSR was performed (Kouremeti et al., 2015)
13 and showed that the instrument was stable in the 2-year dataset of MOL-RAO, demonstrating
14 a mean difference of 0.3% with maximum of 4% in some channels. In addition, comparison
15 with different CIMEL instruments for longer periods in all cases showed differences smaller
16 than 0.03 at AOD at visible and near infrared wavelengths (Kouremeti and Gröbner, 2014).
17 So, the AOD related uncertainty calculated in all studies for the PSR is in at maximum 0.03.
18 Rayleigh optical depths in this spectral region are very low (~ 0.01 for 1000 mb pressure) and
19 the uncertainty is 1% (Teillet, 1990) and, thus, we may consider it negligible for the IWV
20 retrieval. Air masses were calculated using the formula found in Kasten (1966), which
21 assumes a standard vertical profile of humidity in the troposphere and introduces an error of
22 10% at SZA higher than 85°, due to variations in real atmospheric conditions but is negligible
23 for SZA lower than 75° (Tomasi et al., 1998).
24 Coefficients a, b, c derived from fitting of MODTRAN outputs introduce an uncertainty that is
25 related to the goodness of the calculated fit. For the monochromatic approach at 946nm,
26 Root Mean Square Error (RMSE) is 0.0021 and for the spectral approach at window 934-
27 948nm it is 0.0029. So, the uncertainties introduced using the empirical equation to estimate
28 IWV from T_w is 0.2% and 0.3% for each approach accordingly, due to the fitting.
29 Uncertainty is also introduced by the extrapolation of AOD from the 865 nm and lower
30 wavelength region to water absorbing wavelengths in the range of 934-948 nm. A sensitivity



1 analysis of the IWV retrieval in respect to fluctuations in AOD caused by the uncertainty of
2 AOD was performed. The uncertainty of this extrapolation was calculated to be 0.03.
3 Figure 7 shows the total expected uncertainty of IWV retrieval with respect to SZA, for the
4 case of AOD=0.3 at 865 nm and the case of IWV equal to 2 cm. Highest uncertainties are
5 expected for higher than 75° SZA, when IWV is very low or AOD very high. Very low IWV values
6 could be found only at very dry atmospheres and even then, those are rarely below 0.2 cm.
7 In the range of values found in the dataset of MOL-RAO (0.3 - 4.5cm), the maximum
8 uncertainty is 0.28cm. For the 0.3 - 0.5cm values in our dataset, absolute uncertainty is
9 calculated as 0.08-0.12 cm. Thus, the maximum expected uncertainty of the method, using
10 PSR instruments, is found at the range of 15%, when the solar zenith angle is very high
11 (SZA>75°) and AOD higher than 0.9.



12
13 **figure 7.** Uncertainty (%) of IWV retrieved using monochromatic approach at 946 nm, for
14 various Solar Zenith Angles (°) test figure, in respect to AOD (when IWV=2cm) in upper plot,
15 and with respect to IWV (when AOD=0.3) in lower plot.

16
17
18
19
20

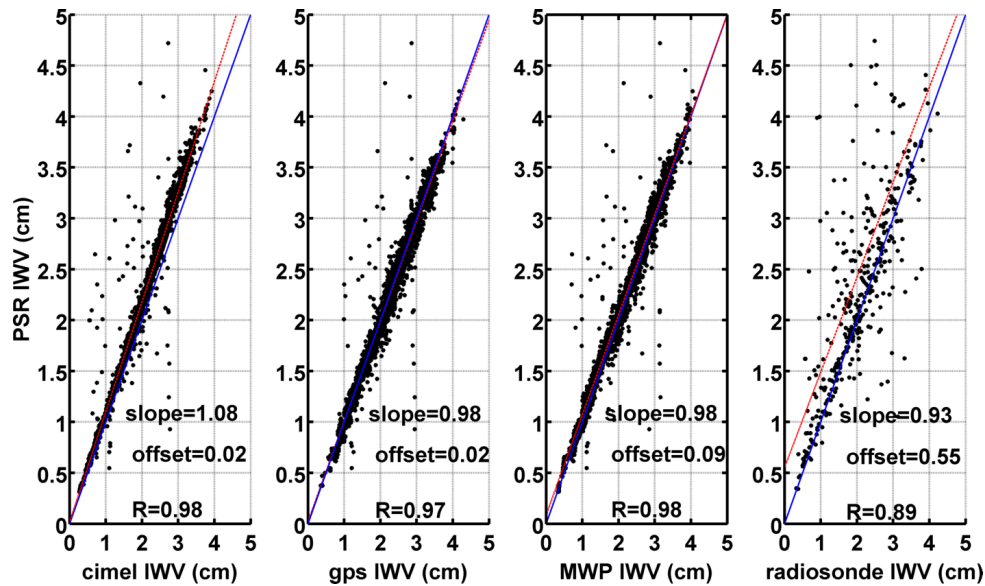


1 5. Results

2

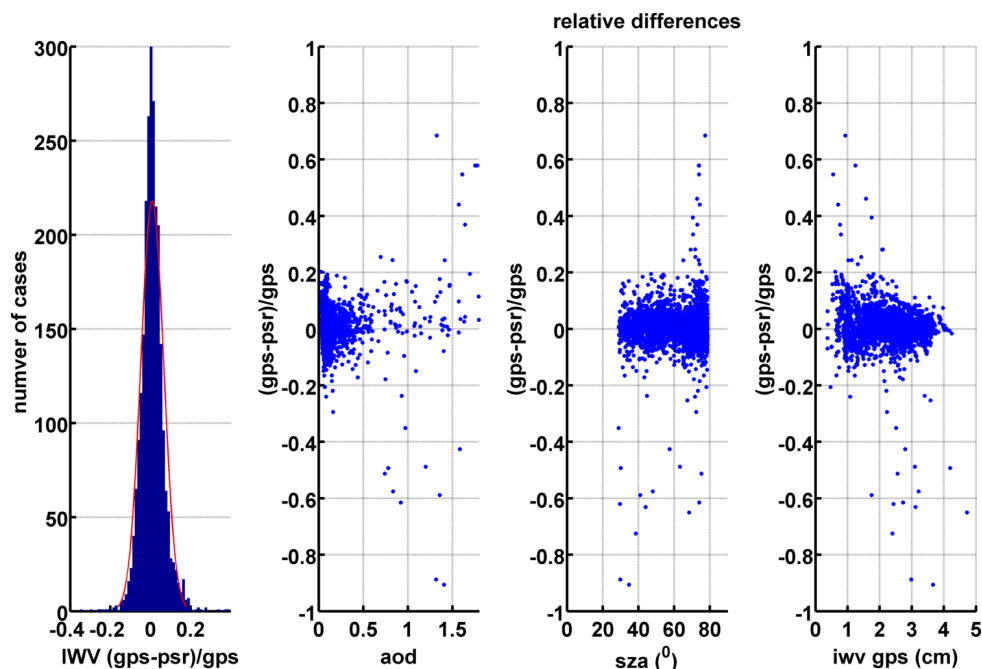
3 In order to validate the results retrieved from both methodologies, we have used the various
4 IWV datasets recorded at MOL-RAO. Calculations have been performed for all PSR
5 measurements, but we have used only the ones synchronous to CIMEL level data in order to
6 avoid cloud contamination (Smirnov et al., 2000). So indirectly the AERONET cloud screening
7 procedure has been used. For each CIMEL data point we have calculated the synchronous PSR
8 value by averaging all values in a ± 5 min interval. This approach produced a dataset of 3501
9 synchronous data points between PSR and CIMEL, 2507 between PSR and GPS and 2964
10 between PSR and MWP. For radiosondes, in order to have a robust coincidence criterion, we
11 have followed the approach of Schneider et al. (2010) averaging PSR measurements for ± 20
12 min from the time that the radiosonde reaches a 4 km height, in order to minimize spatial
13 and temporal PSR and radiosonde measurement differences.

14 For the monochromatic approach at 946 nm, the comparison is presented in Figure 8 and
15 corresponding statistics in Table 1. Better agreement was found when compared to MWP
16 retrievals, but at similar level as for the comparisons to CIMEL and to GPS retrievals. Mean
17 absolute difference is slightly lower when compared to GPS (0.02 cm), but the spread of the
18 differences is almost the same for CIMEL, GPS and MWP (standard deviation between 0.16
19 cm and 0.18 cm). Differences with CIMEL retrieval are within the CIMEL uncertainty range. It
20 appears that PSR overestimates the IWV compared to CIMEL for IWV larger than 3 cm, which
21 causes the different slope in the graphs. This feature is not shown in the comparison with GPS
22 and MWP at these IWV values. Schneider et al. (2010) also observed a different behavior of
23 CIMEL retrievals as compared to other methods, regarding dry or wet conditions in the
24 atmosphere and linked to filter characterization errors. Radiosonde retrievals had largest
25 deviations and more scattered differences, which is expected because of the different
26 temporal and spatial scale of the RS retrieval. Percentiles 10-90 of the differences are also
27 presented in table 1 and GPS, MWP and CIMEL retrievals have a spread of differences in the
28 range of the uncertainties described for these instruments. In general RS retrievals
29 demonstrate the most spread differences from the PSR retrievals, though the average and
30 median are in the uncertainty range of the instruments. The high spread of the differences is
31 explained by the random error introduced by the temporal variability of IWV in the time range
32 averaged and by the different paths of the sounding.



1
 2 **Figure 8:** IWV retrievals from PSR using monochromatic approach at 946 nm compared to
 3 synchronous ones of CIMEL, GPS, MWP and radiosonde, for the full 2-years measuring period.

4
 5 A histogram of relative difference of this retrieval compared to GPS is demonstrated in Figure
 6 8. Also, IWV retrievals relative differences are shown against other parameters (AOD, SZA and
 7 IWV from GPS). A normal distribution with mean at 0.024 cm and standard deviation of 0.084
 8 is fitted to the differences and passed the One-sample Kolmogorov-Smirnov test (Marsaglia
 9 et al., 2003). Thus 95% of the absolute differences are lower than 0.16cm. IWV differences
 10 against AOD at 865 nm show that almost all absolute relative differences higher than 0.2 cm
 11 (20%) are linked to AOD values higher than 0.5. This pattern could be connected to the higher
 12 error introduced by the extrapolation of AOD at 946 nm using different wavelengths.
 13 Furthermore, it appears that most of the large differences appear at high SZA, but there are
 14 also some individual points showing large differences at lower SZA that could be linked to
 15 AOD uncertainty. Compared to IWV retrieved from the GPS it appears that extreme
 16 differences are linked to overestimation from PSR when the absolute value is above 2 cm, and
 17 to underestimation when below , though GPS retrievals are not optimal at more dry
 18 conditions (Schneider et. al., 2010).



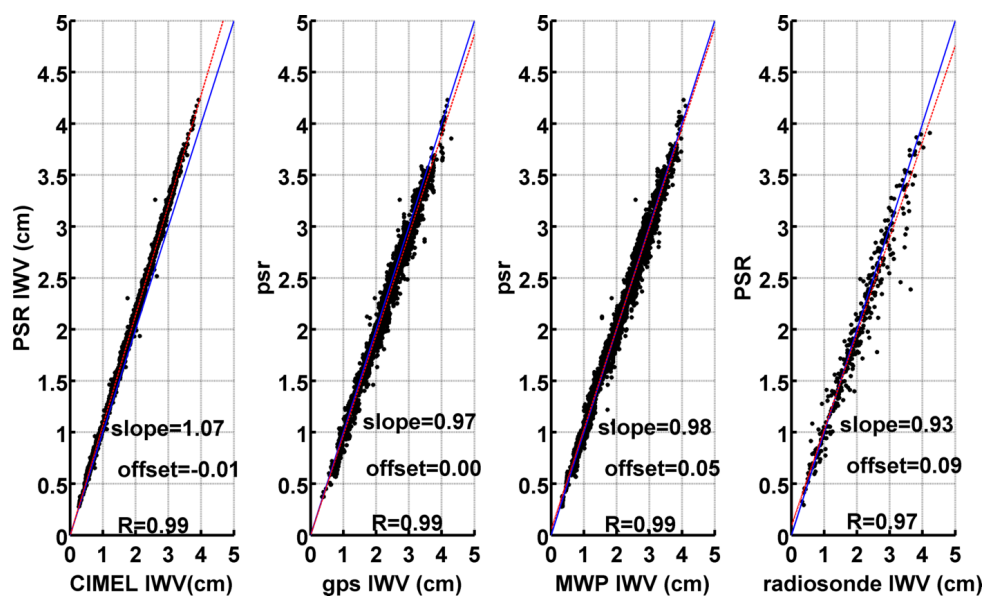
1
 2 **figure 9.** Histogram of *relative difference among synchronous GPS and PSR retrievals – using*
 3 *monochromatic approach at 946 nm- and plotted against AOD (retrieved from PSR at 865*
 4 *nm), solar zenith angle and IWV (retrieved from GPS).*

5
 6
 7
 8 Comparison of the PSR spectral method with other instruments is presented in Figure 10 and
 9 corresponding statistics in Table 2. It is clear that the spread of differences with all methods is
 10 significantly lower than for the monochromatic approach. All comparisons are found with R^2
 11 between 0.96 and 0.98. CIMEL seems to underestimate, compared to this method, but also
 12 compared with the other instruments at higher IWV values. Although the slope caused by the
 13 overestimation is still presented in this approach, the spread of the differences among CIMEL
 14 and PSR retrievals is significantly lower than any other comparison, with $\sigma=0.07$ and 10-90
 15 percentiles of differences in a range of -0.23–0.02. Differences with GPS and MWP retrievals
 16 have the same spread and statistical behavior. Radiosonde data are in significantly better
 17 agreement with the spectral approach retrieval than with the monochromatic approach.
 18 Standard deviation of the differences is at least halved as compared to the monochromatic



1 approach and all mean relative differences when compared to any other instrument are lower
 2 than 0.7%. Comparison with RS' dataset has still significantly larger standard deviation than
 3 other comparisons but it is less than 1/4 of the the monochromatic approach's. Extreme
 4 values observed with the monochromatic approach are significantly reduced and the
 5 standard deviation is reduced to values from 0.07 for CIMEL to 0.18 for RS retrievals. A wider
 6 spread is observed at higher SZA, which is explained by the increase of the instrument related
 7 uncertainty at these angles.

8



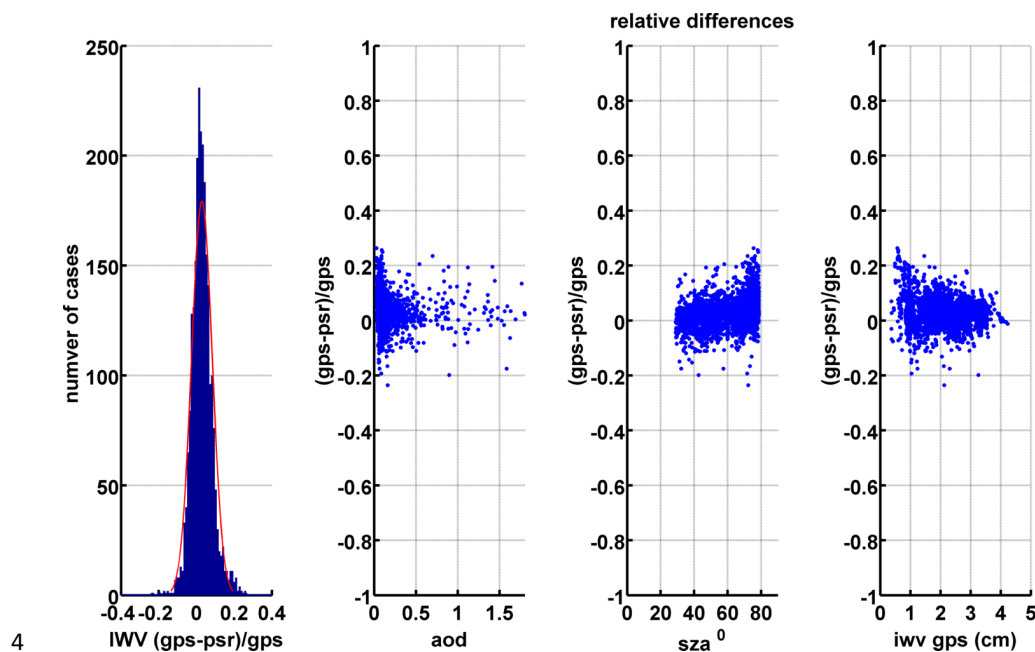
9

10 **Figure 10** IWV retrievals from PSR using spectral approach at 934-948 nm region, compared
 11 to synchronous ones of CIMEL, GPS, MWP and radiosonde, for the full 2-year measuring
 12 period.

13 Figure 11 displays a histogram of relative differences of the spectral approach for the spectral
 14 window 934-948 nm the GPS dataset and a relative IWV comparison against: AOD at 865nm,
 15 SZA and GPS' IWV. A normal distribution with mean at 0.021cm and σ at 0.042 is fitted at the
 16 data, passed the One-sample Kolmogorov-Smirnov test (Marsaglia et al., 2003) and 95% of
 17 differences are lower than 0.08 cm. The quality of spectral retrieval shows no dependence
 18 on absolute IWV values, as the distribution of differences in figure 11 is independent of IWV.
 19 When the IWV relative difference is shown against AOD, higher relative differences than 0.1
 20 are more frequent for AOD lower than 0.2.



- 1 Median differences and 10-90 percentiles.
- 2
- 3



4
5 **figure 11.** Relative difference among synchronous GPS and PSR retrievals – using spectral
6 approach at 934-948nm region- plotted against (a) AOD (retrieved from PSR at 865nm), (b)
7 solar zenith angle and (c) IWV (retrieved from GPS).

10 6. Conclusions

11 The aim of this study was to develop methodologies and tools in order to retrieve IWV from
12 PSR spectral measurements. The methods which were developed can be applied to provide
13 long term time-series of IWV using any direct sun spectroradiometer able to measure at the
14 930-950 spectral range.

15 Two approaches to retrieve IWV from PSR spectral direct solar irradiance measurements
16 have been developed. The first one is the monochromatic approach using an individual
17 wavelength, and the second uses a spectral window. For both methods the corresponding
18 Water Vapor Transmittance has been retrieved from the PSR measurements, from which IWV



1 can be calculated using a three-parameter formula following the principles of Ingold's (2000)
2 work.
3 The dependence of the retrievals to other parameters has been investigated for both
4 approaches, and found to be affected in cases of low (<0.2) AOD coincidences. Larger
5 deviations were observed at high Solar Zenith Angles, which are linked to higher uncertainties
6 in those retrievals.
7 Comparisons to other instruments (CIMEL, MWP) and methods (GPS, radiosondes) have been
8 performed to select the optimum wavelength and spectral window for the IWV retrieval of
9 the PSR. All the channels in the infrared region of 900-950 nm were tested for
10 monochromatic approach and 946 nm bandpass was selected as giving significantly better
11 results than other channels. For the spectral approach all possible spectral windows limits
12 combinations were tested and the spectral window of 934-948 nm was finally chosen.
13 Uncertainties of the methodologies have been investigated and in more frequent
14 atmospheric conditions have been found less than 5%, while might reach up to 15% in cases
15 of very high AOD, very low IWV and SZA higher than 75° combined. In general, absolute
16 uncertainty is found to be in the range of 0.08-0.3 cm.
17 Retrievals from a 2-year long time-series at MOL-RAO in Lindenberg, Germany showed that
18 the monochromatic approach had differences in the order of 0.4% compared to GPS and
19 MWP, in the order of 2.7% compared to RS, and 3.3% compared to CIMEL. 95% of differences
20 with GPS retrievals are less than 0.15 cm.
21 Spectral approach's retrievals showed better agreement with other datasets, having
22 differences of 0.7% compared to CIMEL, 0.4% compared to GPS, 0.3% compared to MWP, and
23 0.5% when compared to RS. Also, the differences to other retrievals were always at least half
24 spread compared to monochromatic approach. Differences with GPS retrievals were less than
25 0.08cm in 95% of the dataset. Differences among the other instruments found independent
26 of other variables, suggesting robust appliance of the method.
27 Overall, the accuracy of IWV retrieval is in the same order of the other well established
28 methods and devices. The spectral approach, benefiting from the characteristics of PSR,
29 provided statistically better results. Also, having applied the method to a 2-year dataset,
30 indicated a stable long-term performance of the instrument, which shows that it can be used
31 for IWV calculations. The IWV method development and assessment presented in this work
32 provides an added value to the PSR instrument, being able to measure simultaneously



1 spectral solar irradiance components (direct and horizontal), aerosol spectral optical
2 properties (AOD, Angstrom Exponents) and IWV, constituting the PSR as a unique sun-
3 photometric instrument.

4

5 **7.References**

6 Alexandrov, M.D., Schmid, B., Turner, D.D., Cairns, B., Oinas, V., Lacis, A.A., Gutman, S.I.,
7 Westwater, E.R., Smirnov, A. and Eilers, J., Columnar water vapor retrievals from
8 multifilter rotating shadowband radiometer data. *Journal of Geophysical Research:*
9 *Atmospheres*, 114(D2), 2009.

10 American Meteorological Society, Precipitable Water Vapor, Glossary of Meteorology, 2015.

11 Beyrich, F., and W. K. Adam, Site and Data Report for the Lindenberg Reference Site in CEOP
12 - Phase I. *Berichte des Deutschen Wetterdienstes*, 230, Offenbach am Main, Germany,
13 55 pp, 2007.

14 Berk, A., Bernstein, L.S. and Robertson, D.C., MODTRAN: A moderate resolution model for
15 LOWTRAN (No. SSI-TR-124). SPECTRAL SCIENCES INC BURLINGTON MA, 1987.

16 Berk, A., Anderson, G.P., Bernstein, L.S., Acharya, P.K., Dothe, H., Matthew, M.W., Adler-
17 Golden, S.M., Chetwynd Jr, J.H., Richtsmeier, S.C., Pukall, B. and Allred, C.L., MODTRAN
18 4 radiative transfer modeling for atmospheric correction. In *Proceedings of SPIE- The*
19 *International Society for Optical Engineering* (Vol. 3756, pp. 348-353),1999.

20 Bevis, M., S. Businger, T. A. Herring, C. Rocken, R. A. Anthes, and R. H. Ware. "GPS
21 Meteorology: Remote Sensing of Atmospheric Water Vapor Using the Global Positioning
22 System." *Journal of Geophysical Research*, Vol. 97, No. D14, , pp. 15,787-15,801, October
23 20, 1992

24 Bock, O., Bossler, P., Pacione, R., Nuret, M., Fourrié, N. and Parracho, A. : A high-quality
25 reprocessed ground-based GPS dataset for atmospheric process studies, radiosonde and
26 model evaluation, and reanalysis of HyMeX Special Observing 30 Period. *Q.J.R. Meteorol.*
27 *Soc.*, 142: 56–71. doi:10.1002/qj.2701, 2016.



- 1 Bodhaine, B. A., Wood, N. B., Dutton, E. G., and Slusser, J. R.: On Rayleigh optical depth
2 calculations, *J. Atmos. Ocean. Tech.*, 16(11), Part 2, pp 1854–1861, 1999.
- 3 Cadeddu, M. P., J. C. Liljegren, and D. D. Turner, The Atmospheric Radiation Measurement
4 (ARM) program network of microwave radiometers: Instrumentation, data and
5 retrievals, *Atmos. Meas. Tech.*, 6, 2359–2372, doi:10.5194/amt-6-2359-2013, 2013.
- 6 Campanelli, M., Estellés, V., Smyth, T., Tomasi, C., Martínez- Lozano, M. P., Claxton, B., Muller,
7 P., Pappalardo, G., Pietruczuk, A., Shanklin, J., Colwell, S., Wrench, C., Lupi, A., Mazzola,
8 M., Lanconelli, C., Vitale, V., Congeduti, F., Dionisi, D., and Cacciani, M.: Monitoring of
9 Eyjafjallajökull volcanic aerosol by the new European SkyRad users (ESR) sun-sky
10 radiometer network, *Atmos. Environ.*, 48, 33–45, 2012.
- 11 Campanelli, M., Nakajima, T., Khatri, P., Takamura, T., Uchiyama, A., Estellés Leal, V., Liberti,
12 G.L. and Malvestuto, V., Retrieval of characteristic parameters for water vapour
13 transmittance in the development of ground based sun-sky radiometric measurements
14 of columnar water vapour. *Atmospheric Measurement Techniques*, 2014, num. 7, p.
15 1075-1087, 2014.
- 16 Che, H., Gui, K., Chen, Q., Zheng, Y., Yu, J., Sun, T., Zhang, X. and Shi, G., Calibration of the 936
17 nm water-vapor channel for the China aerosol remote sensing NETWORK (CARSNET) and
18 the effect of the retrieval water-vapor on aerosol optical property over Beijing, China.
19 *Atmospheric Pollution Research*, 7(5), pp.743-753, 2016.
- 20 Eck, T. F., Holben, B. N., Ward, D. E., Mukelabai, M. M., Dubovik, O., Smirnov, A., Schafer, J. S.,
21 Hsu, N. C., Piketh, S. J., Queface, A., and Roux, J. L.: Variability of biomass burning aerosol
22 optical characteristics in southern Africa during the SAFARI 2000 dry season campaign
23 and a comparison of single scattering albedo estimates from radiometric measurements,
24 *J. Geophys. Res.-Atmos.*, 108, 2156–2202, doi:10.1029/2002JD002321, 2003.
- 25 Gröbner, J., Kazadzis, S., Kouremeti, N., Doppler, L., Tagirov, R. and Shapiro, A.I., February.
26 Spectral solar variations during the eclipse of March 20th, 2015 at two European sites.
27 In *AIP Conference Proceedings* (Vol. 1810, No. 1, p. 080008). AIP Publishing, 2017a.



- 1 Gröbner, J., Kröger, I., Egli, L., Hülsen, G., Riechelmann, S., and Sperfeld, P.: The high-
2 resolution extraterrestrial solar spectrum (QASUMEFTS) determined from ground-based
3 solar irradiance measurements, Atmos. Meas. Tech., 10, 3375-3383,
4 <https://doi.org/10.5194/amt-10-3375-2017>, 2017b.
- 5 Gröbner, J., Kouremeti, N., Coulon, E., Durig, F., Gyo, M., Soder, R., Wasser, D.,
6 Spectroradiometer for Spectral Aerosol Optical Depth and Solar Irradiance
7 Measurements, annual report PMOD/WRC, page 13,
8 http://pmodwrc.ch/annual_report/2012_PMODWRC_Annual_Report.pdf, 2012.
- 9 Gröbner, J., Kouremeti, N., Nevas, S., Blattner, P., Characterisation Studies of Precision Solar
10 Spectroradiometer, PMOD-WRC Annual Report 2014, p26
11 http://pmodwrc.ch/annual_report/2014_PMODWRC_Annual_Report.pdf, 2014
- 12 Güldner, J.: A model-based approach to adjust microwave observations for operational
13 applications: results of a campaign at Munich Airport in winter 2011/2012, Atmos. Meas.
14 Tech., 6, 2879-2891, doi:10.5194/amt-6-2879-2013, 2013.
- 15 Güldner, J. and Spänkuch, D., Remote sensing of the thermodynamic state of the atmospheric
16 boundary layer by ground-based microwave radiometry. Journal of Atmospheric and
17 Oceanic Technology, 18(6), pp.925-933, 2001.
- 18 GAW Report-No 231, Fourth WMO Filter Radiometer Comparison (FRC-IV) 28 September-16
19 October 2015; Davos, Switzerland,
20 https://library.wmo.int/opac/doc_num.php?explnum_id=3369, WMO, 2016
- 21 Hartmann, D., Klein Tank, A., Rusticucci, M., Alexander, L., Brönnimann, S., Charabi, Y.,
22 Dentener, F., Dlugokencky, E., Easterling, D., Kaplan, A., Soden, B., Thorne, P., Wild, M.,
23 and Zhai, P.: Observations: Atmosphere and Surface, in: Climate Change 2013: The
24 Physical Science Basis. Contribution of Working Group I to the Fifth Assessment Report
25 of the Intergovernmental Panel on Climate Change, edited by Stocker, T., Qin, D.,
26 Plattner, G., Tignor, M., Allen, S., Boschung, J., Nauels, A., Xia, Y., Bex, V., and Midgley,
27 P., Cambridge University Press, Cambridge, United Kingdom and New York, NY, USA,
28 2013.



- 1 Hong L., Yunchanga C., Xiaominb W., Zhifangb X., Haishena W., Henga H., Meteorological
2 applications of precipitable water vapor measurements retrieved by the national GNSS
3 network of China, *Geodesy and Geodynamics*, vol 6 no 2, 135-142.
4 <http://dx.doi.org/10.1016/j.geog.2015.03.001>, 2015.
- 5 Holben, B.N., Eck, T.F., Slutsker, I., Tanre, D., Buis, J.P., Setzer, A., Vermote, E., Reagan, J.A.,
6 Kaufman, Y.J., Nakajima, T. and Lavenu, F., 1998. AERONET—A federated instrument
7 network and data archive for aerosol characterization. *Remote sensing of environment*,
8 66(1), pp.1-16.
- 9 Ingold, T., Schmid, B., Matzler, C., Demoulin, P., & Kampfer, N, Modeled and empirical
10 approaches for retrieving columnar water vapor from solar transmittance
11 measurements in the 0.72, 0.82, and 0.94 μ m absorption bands. *Journal of*
12 *Geophysical Research.*, 105(D19), 24327–24343. <http://doi.org/10.1029/2000JD900392>,
13 2000.
- 14 Kasten, F., A new table and approximation formula for the relative optical air mass. *Archiv für*
15 *Meteorologie, Geophysik und Bioklimatologie*, Serie B, 14(2), pp.206-223, 1965.
- 16 Kouremeti, N., Gröbner, J., Spectral Aerosol Optical Depth from a Precision
17 Spectroradiometer, PMOD-WRC Annual Report 2012, p33
18 http://pmodwrc.ch/annual_report/2012_PMODWRC_Annual_Report.pdf, 2012
- 19 Kouremeti, N., Gröbner, J., Spectral Aerosol Optical Depth From a Precision Solar
20 Spectroradiometer During Three Field Campaigns, PMOD-WRC Annual Report 2014, p30
21 http://pmodwrc.ch/annual_report/2014_PMODWRC_Annual_Report.pdf, 2014
- 22 Kouremeti, N., Gröbner, J., Doppler, L., Stability of the Precision Solar Spectroradiometer,
23 PMOD-WRC Annual Report 2015, p40
24 http://pmodwrc.ch/annual_report/2015_PMODWRC_Annual_Report.pdf, 2015
- 25 Marsaglia, G., W. Tsang, and J. Wang. "Evaluating Kolmogorov's Distribution." *Journal of*
26 *Statistical Software*. Vol. 8, Issue 18, 2003.



- 1 Miloshevich, L.M., Vömel, H., Whiteman, D.N. and Leblanc, T., Accuracy assessment and
2 correction of Vaisala RS92 radiosonde water vapor measurements. *Journal of*
3 *Geophysical Research: Atmospheres*, 114(D11), 2009
- 4 Nyeki, S., Vuilleumier, L., Morland, J., Bokoye, A., Viatte, P., Mätzler, C., & Kämpfer, N. , A 10-
5 year integrated atmospheric water vapor record using precision filter radiometers at two
6 high-alpine sites. *Geophysical Research Letters*, 32(23), 1–4,
7 <http://doi.org/10.1029/2005GL024079> , 2005.
- 8 Pratt, R.W., Review of radiosonde humidity and temperature errors. *Journal of Atmospheric*
9 *and Oceanic Technology*, 2(3), pp.404-407, 1985.
- 10 Reichard, J., U. Wandinger, M. Serwazi, and C. Weitkamp , Combined Raman lidar for aerosol,
11 ozone and moisture measurements, *Opt. Eng.*, 35, 1457–1465, 1996.
- 12 Schneider, M., Romero, P. M., Hase, F., Blumenstock, T., Cuevas, E., & Ramos, R., Continuous
13 quality assessment of atmospheric water vapour measurement techniques: FTIR, Cimel,
14 MFRSR, GPS, and Vaisala RS92. *Atmospheric Measurement Techniques*, 3(2), 323–338.
15 <http://doi.org/10.5194/amt-3-323-2010,2010>.
- 16 Schmid, B., Michalsky, J.J., Slater, D.W., Barnard, J.C., Halthore, R.N., Liljegren, J.C., Holben,
17 B.N., Eck, T.F., Livingston, J.M., Russell, P.B. and Ingold, T., Comparison of columnar
18 water-vapor measurements from solar transmittance methods. *Applied Optics*, 40(12),
19 pp.1886-1896, 2001.
- 20 Smirnov, A., Holben, B.N., Eck, T.F., Dubovik, O. and Slutsker, I., Cloud-screening and quality
21 control algorithms for the AERONET database. *Remote Sensing of Environment*, 73(3),
22 pp.337-349, 2000.
- 23 Smirnov, A, Holben, B.N., Lyapustin A., Slutsker, I. and Eck, T.F., AERONET processing
24 algorithms refinement, AERONET Workshop, El Arenosillo, Spain , May 10 - 14, 2004.
- 25 Soden, B.J. and Held, I.M., An assessment of climate feedbacks in coupled ocean–atmosphere
26 models. *Journal of Climate*, 19(14), pp.3, 2006.



- 1 Soden, B. J., and J. R. Lanzante, An assessment of satellite and radiosonde climatologies of
2 upper-tropospheric water vapor, *J. Climate*, 9, 1235–1250, 1996.
- 3 Teillet, P.M., Rayleigh optical depth comparisons from various sources. *Applied Optics*,
4 29(13), pp.1897-1900.354-3360, 1990.
- 5 Tomasi, C., Vitake, V. and De Santis, L.V., Relative optical mass functions for air, water vapour,
6 ozone and nitrogen dioxide in atmospheric models presenting different latitudinal and
7 seasonal conditions. *Meteorology and Atmospheric Physics*, 65(1), pp.11-30, 1998.
- 8 Vömel, H., Selkirk, H., Miloshevich, L., Valverde-Canossa, J., Valdés, J., Kyrö, E., Kivi, R., Stolz,
9 W., Peng, G. and Diaz, J.A., Radiation dry bias of the Vaisala RS92 humidity sensor.
10 *Journal of Atmospheric and Oceanic Technology*, 24(6), pp.953-963, 2007.
- 11 Ware, R., Carpenter, R., Güldner, J., Liljegren, J., Nehr Korn, T., Solheim, F.,
12 and Vandenberghe, F.: A multi-channel radiometric profiler of temperature, humidity
13 and cloud liquid, *Radio Sci.*, 38, 8079, doi:10.1029/2002RS002856, 2003.
- 14 Wang, J., Zhang, L., Dai, A., Van Hove, T., and Van Baelen, J.: A near-global, 2-hourly dataset
15 of atmospheric precipitable water from ground-based GPS measurements, *J. Geophys.*
16 *Res.*, 112, D11107, doi:10.1029/2006JD007529, 2007.
- 17 Westwater, E. R., Crewell, S., Mätzler, C., and Cimini, D.: Principles of surface-based
18 microwave and millimeter wave radiometric remote sensing of the troposphere,
19 *Quaderni della Società Italiana di Elettromagnetismo*, 1, 50–90, 2005.
- 20 WMO/GAW: Experts workshop on Global Surface-based Network for long term
21 observations of column aerosol optical properties, Davos, Switzerland, 8–10 March 2004.
22 GAW report No. 162, WMO TD No. 1287, 153 pp., available at:
23 <http://www.wmo.int/pages/prog/arep/gaw/gaw-reports.html> (last access: 21 October
24 2016), 2005,
- 25 Yu, S., Alapaty, K., Mathur, R., Pleim, J., Zhang, Y., Nolte, C., Eder, B., Foley, K. and Nagashima,
26 T., Attribution of the United States “warming hole”: Aerosol indirect effect and
27 precipitable water vapor. *Scientific reports*, 4, 2014.



1

2 *Table 1. Statistics of differences among retrievals from PSR using Monochromatic Approach*
 3 *at 946 nm, and retrievals from other instruments for the whole dataset.*

	<i>N</i>	<i>MEAN</i> <i>(CM)</i>	<i>STANDARD</i> <i>DEVIATION</i>	<i>MEDIAN</i> <i>(CM)</i>	<i>PERCENTILE</i> <i>10-90</i>	<i>MEAN RELATIVE (%)</i>	<i>R</i> ²
CIMEL	3501	-0.16	0.18	-0.14	-0.30 -0.04	-3.3	0.92
GPS	2507	0.01	0.17	0.01	-0.11 0.14	0.4	0.94
MWP	2964	-0.05	0.17	-0.04	-0.16 0.07	-0.4	0.95
RS	414	-0.41	1.03	-0.10	-1.42 0.22	-2.7	0.79

4

5



1 **Table 2.** *Statistics of differences among retrievals from PSR using Spectral Approach at 934-*
 2 *948 nm window, and retrievals from other instruments for the whole dataset.*

	N	MEAN (CM)	STANDARD DEVIATION	MEDIAN (CM)	PERCENTILE 10-90	MEAN RELATIVE (%)	R ²
CIMEL	3501	-0.11	0.07	-0.10	-0.23 -0.02	-0.7	0.97
GPS	2507	0.05	0.10	0.04	-0.06 0.18	0.4	0.97
MWP	2964	-0.04	0.10	0.01	-0.12 0.12	0.3	0.98
RS	414	0.04	0.18	0.02	-0.13 0.25	0.5	0.95

3

4



1

2

3 Lexicon

4

AERONET	AERosol RObotic NETwork
AOD	Aerosol Optical Depth
CIMEL	Sunphotometer Cimel CE318 used in AERONET network
DWD	Deutscher Wetterdienst (German Meteorological Service)
GPS	Global Positioning System
IWV	Integrated Water Vapor (water vapor column)
MODTRAN RTM	MODerate resolution atmospheric TRANsmisssion Radiative Transfer Model
MOL-RAO	Meteorologisches Observatorium Lindenberg – Richard Assmann Observatorium
MWP	Microwave Radiometer Profiler
PMOD/WRC	Physikalisch-Meteorologisches Observatorium Davos / World Radiation Center
PFR	Precision Filter Radiometer
PSR	Precision Solar spectroRadiometer
RH	Relative Humidity
RS	Meteorological Radiosondes
WMO	World Meteorological Organisation

5